

# Carvacrol Alleviates Hyperuricemia-Induced Oxidative Stress and Inflammation by Modulating the NLRP3/NF- $\kappa$ B Pathway

Muhammad Riaz<sup>1</sup>, Lina Tariq Al Kury<sup>2</sup>, Noreen Atzaz<sup>3</sup>, Abdullah Alattar<sup>4</sup>, Reem Alshaman<sup>4</sup>, Fawad ali Shah<sup>1</sup>, Shupeng Li<sup>5</sup>

<sup>1</sup>Riphah Institute of Pharmaceutical Sciences, Riphah International University, Islamabad, Pakistan; <sup>2</sup>Department of Natural and Health Sciences Zayed University, Abu Dhabi, United Arab Emirates; <sup>3</sup>Department of Pathology, Benazir Bhutto Hospital, Rawalpindi, Pakistan; <sup>4</sup>Department of Pharmacology and Toxicology, Faculty of Pharmacy, University of Tabuk, Tabuk, Kingdom of Saudi Arabia; <sup>5</sup>State Key Laboratory of Oncogenomics, School of Chemical Biology and Biotechnology, Peking University Shenzhen, Shenzhen, People's Republic of China

Correspondence: Fawad ali Shah; Shupeng Li, Email fawad.shah@riphah.edu.pk; lisp@pkusz.edu.cn

**Purpose:** Gouty arthritis is generally induced by the accumulation of monosodium urate (MSU) crystals in the joints due to elevated serum uric acid levels, potentially leading to serious pathological disorders such as nephrolithiasis, renal failure, and acute gouty arthritis. In this study, we aimed to validate the anti-gout effects of carvacrol, a phenolic monoterpene.

**Materials and Methods:** Male Sprague–Dawley rats were divided into normal saline, disease group by injecting potassium monooxalate (PO) at a dose of 250 mg/kg, and three treatment groups, either with carvacrol 20 mg/kg or 50 mg/kg and 10 mg/kg allopurinol. The blood and tissue samples were subsequently collected and analyzed using different biochemical and histopathological techniques.

**Results:** Our results revealed a significant increase in the serum levels of oxidative stress-related markers, namely, uric acid and C-reactive protein (CRP), and NLRP3 inflammasome-dependent inflammatory mediators, including nuclear factor kappa B (NF- $\kappa$ B) and tumor necrosis factor-alpha (TNF- $\alpha$ ). Carvacrol administration for seven consecutive days exhibited significant anti-hyperuricemic and anti-inflammatory effects in a dose-dependent manner. Notably, the 50 mg/kg carvacrol treatment was observed to produce results similar to the allopurinol treatment. Furthermore, the renal safety of carvacrol was confirmed by the renal function test.

**Conclusion:** Carvacrol potentially alleviates hyperuricemia-induced oxidative stress and inflammation by regulating the ROS/NLRP3/NF- $\kappa$ B pathway, thereby exerting protective effects against joint degeneration.

**Keywords:** hyperuricemia, gout, inflammation, NLRP3, monosodium urate crystals

## Introduction

Hyperuricemia is a common biochemical disorder characterized by the increase in serum uric acid levels (up to 7.2 mg/dl) caused by either increased production or a decreased elimination of uric acid from the body.<sup>1</sup> The number of hyperuricemia-related diseases is increasing worldwide, which can be linked to various genetic and environmental factors, including stressful environments and bad dietary habits.<sup>2</sup> It is difficult to estimate the global prevalence of gout accurately owing to a lack of data for many countries. It is more prevalent in the male population as compared to females and ranges from a prevalence of <1% to 6.8% and an incidence of 0.58–2.89 per 1000 person-years.<sup>3</sup> Another study suggests that 1.4 females and 4 males in every 1000 population are affected by gout annually.<sup>4</sup> Hyperuricemia can sometimes lead to different pathological disorders, such as gout, acute gouty arthritis, or chronic rheumatoid arthritis, an inflammatory autoimmune disease of the joints.<sup>5</sup> Since uric acid is a resultant metabolite of purine oxidation and a purine-rich diet can exacerbate uric acid precipitation. Moreover, a deficiency of the enzyme hypoxanthine phosphoribosyltransferase (HPRT), a rate-limiting enzyme in purine synthesis, promotes the degradation of purine to uric acid during purine metabolism, leading to medical conditions such as hemolysis and

rhabdomyolysis.<sup>6</sup> When serum uric acid accumulates in the peripheral joints as monosodium urate (MSU) crystals, the body's immune response may result in several variants of gout, such as acute gouty arthritis, gouty arthropathy, uric acid urolithiasis, gouty nephropathy, and nephrolithiasis.<sup>7</sup> Furthermore, previous studies found that hyperuricemia is a risk factor for diabetes mellitus, cardiovascular diseases, and chronic renal failure.<sup>8–10</sup> Several studies also established a direct link between hyperuricemia and obesity or hypertension.<sup>11,12</sup> However, despite being common human disorders, gout and hyperuricemia remain poorly managed due to limited therapeutic options that require both urate-lowering agents and anti-inflammatory drugs.<sup>13</sup> Urate level can be reduced using xanthine oxidase inhibitors (eg, allopurinol and febuxostat), which inhibit urate production, or uricosuric agents (eg, probenecid and benzbromarone), which promotes urate excretion.<sup>14</sup> However, these drugs often induce hypersensitivity reactions, interact with other drugs, and cause certain disease pathologies, such as renal injury, thereby limiting their wider application. Furthermore, these medications exert considerable anti-hyperuricemic effects but only have slight anti-inflammatory potential. Thus, new anti-inflammatory and urate-lowering agents are being investigated to improve their efficacy and safety. As a major hallmark of hyperuricemia and gout, combating inflammation is an effective strategy for prevention and treatment.<sup>15</sup> Interestingly, uric acid reportedly exhibits potent antioxidant properties by executing cellular protection.<sup>16</sup> However, several studies reported that urate exacerbates oxidative stress by releasing free radicals and deactivating innate antioxidant enzymes.<sup>17,18</sup> Furthermore, hyperuricemia can trigger inflammation because MSU crystals are involved in activating the NLRP3 inflammasome and interleukin (IL-1) during the pathogenesis of acute gout.<sup>19,20</sup> Previous studies suggested that the NLRP3 inflammasome is an integral component of initiating inflammation in gout.<sup>21</sup> It is a multimeric protein complex that initiates an inflammatory form of cell death and triggers the release of pro-inflammatory cytokines IL-1 $\beta$  and IL-18.<sup>22</sup> In gout, the cytoplasmic NLRP3 inflammasome composed of procaspase 1 and apoptosis-associated speck-like protein (ASC) is used as a predictor of inflammation. Recently, several studies utilizing NLRP3 inhibitors in the treatment of gout revealed significantly favorable results<sup>23–25</sup> suggesting that the NLRP3 inflammasome is a potential target protein for gout therapy. Notably, the release of reactive oxygen species (ROS) and pro-inflammatory mediators, such as IL-1 $\beta$  and tumor necrosis factor- $\alpha$  (TNF- $\alpha$ ), often leads to cellular damage and lipid peroxidation (LPO),<sup>26</sup> while the simultaneous inhibition of COX-2 and TNF- $\alpha$  helps alleviate the symptoms of gouty inflammation.<sup>27</sup> Furthermore, several studies demonstrated that suppressing oxidative stress-induced inflammation can effectively ameliorate gout symptoms. Furthermore, nanoparticles strategies are adopted to ameliorate oxidative stress in gouty pathology.<sup>28,29</sup> Still, the management of hyperuricemia and gout disorders is currently a challenging task and since inflammation is an integral etiological component underlying gout pathogenesis, and therefore it must be considered during the development of treatment strategies.

Natural drug repositories are generally a rich source for new drug development. This fact is acknowledged not only by other researchers but also by our group.<sup>30–32</sup> For example, the phenolic monoterpene carvacrol possesses distinct pharmacological properties, including antioxidant, anti-inflammatory, hepatoprotective, spasmolytic, and anti-cancer activities.<sup>33,34</sup> Furthermore, carvacrol exerts anti-obesity effects, positively regulates cholesterol metabolism, and negatively modulates inflammatory cytokines via numerous pathways.<sup>35</sup> Taking into consideration the pharmacological value of carvacrol and the significance of new drug discovery, the current study aimed to investigate whether carvacrol administration can ameliorate PO-induced hyperuricemia. Our findings may contribute new insights for future research on the prevention and treatment of hyperuricemia and gout.

## Materials and Methods

### Chemicals

Potassium oxonate (catalog# 156124), carvacrol (catalog# W224511) were purchased from Sigma-Aldrich (St. Louis, MO, USA), while allopurinol was obtained from Pharmedic Laboratories (Pvt.) Ltd. (Lahore, Pakistan). The primary antibodies TNF- $\alpha$  (SC-52B83) and nuclear factor-kappa B (p-NF- $\kappa$ B) (SC-271908) and other immunohistochemistry-related consumables, including the Elite ABC kit (SC-2018) and 3,3-diaminobenzidine (DAB; SC-216567), were procured from Santa Cruz Biotechnology (Santa Cruz, CA, USA). The biotinylated secondary antibody (ab-6789) and

DPX mounting media were purchased from Abcam (Cambridge, MA, USA). The enzyme-linked immunosorbent assay (ELISA) kit for rat NLPR3 (CAS# A5652) was purchased from Shanghai MLBIO Biotechnology Co., Ltd. (Shanghai, China), while the ELISA kit for rat TNF- $\alpha$  (Catalog# E-EL-R0019) was obtained from Elabscience (Houston, TX, USA). The kits for uric acid, blood urea nitrogen, creatinine, and C-reactive protein (CRP) were purchased from Beckman Coulter (Brea, CA, USA). All other consumables including formaldehyde, hydrogen peroxide (H<sub>2</sub>O<sub>2</sub>), reduced glutathione (GSH), glutathione S-transferase (GST), catalase, trichloroacetic acid, 1-chloro-2,4-dinitrobenzene (CDNB), ethanol, xylene, and hematoxylin and eosin (H&E) stains were purchased from (Sigma-Aldrich).

## Animals

Seventy healthy male adult Sprague-Dawley rats, weighing  $200 \pm 20$  g and aged 8–12 weeks, were obtained from the local breeding facility of the Riphah International University Islamabad, Pakistan, and randomly divided into five groups (n=14 rats/group). The rats were placed in plastic cages and maintained at room temperature (18–22 °C), with a light and dark cycle of 12 h. Throughout the experiment, the animals were fed with a rat pellet diet *ad libitum* and given free access to tap water. All experimental protocols were approved by the Research and Ethics Committee (REC) of the Riphah Institute of Pharmaceutical Sciences (RIPS), Riphah International University, Pakistan and by following guidelines of the Institute of Laboratory Animal Resources, Commission on Life Sciences University, National Research Council (1996).

## Induction of Hyperuricemia in Rats

Hyperuricemia was induced in rats as previously described.<sup>35</sup> Briefly, the rats were intraperitoneally injected with 250 mg/kg PO, a urate oxidase inhibitor that promotes uric acid synthesis for seven consecutive days.<sup>36</sup>

## Experimental Design and Drug Treatment

During the seven-day treatment, the experimental rats were divided into five groups and administered daily with 1% dimethyl sulfoxide (DMSO) (saline group), 250 mg/kg PO (model group), 20 mg/kg (carvacrol 20 group), 50 mg/kg (carvacrol 50 group), and 10 mg/kg allopurinol (allopurinol group). Carvacrol, allopurinol, and PO were dissolved in normal saline containing 1% DMSO and were administered intraperitoneally (I/P). In all treatment groups, PO was administered initially and then after 1 h either carvacrol or allopurinol was administered. The rats that successfully passed the experimental period were further processed for experimentation. Four rats from the PO-treated group died during the experiment; hence, new rats were added to compensate for the loss. Following the due period, the rats were grouped into either the biochemical or histopathological cohorts (n = 7 per group) for sample collection and subsequent analyses.

## Blood and Tissue Sample Collection

First, the rats were subjected to 8 h fasting before blood collection. Second, on day 1 of treatment, blood samples were collected via the tail vein to measure the baseline serum uric acid, urea, creatinine, and CRP levels. Third, after day 7 of treatment, the rats were anesthetized, and blood samples were collected again via direct cardiac puncture using a 3-mL BD syringe.<sup>37</sup> Fourth, for serum biochemistry, blood (allowed to clot at  $26 \pm 2$  °C) was collected in clotted tubes. Fifth, the serum was extracted by centrifugation at 3000 rpm for 10 min. Finally, all rats were euthanized, and the tissue samples were obtained.

## Serum Biochemistry

The collected blood samples were used to estimate the serum biochemical parameters. Biochemical assays for determining serum urea, creatinine, uric acid, and CRP levels were performed using specific assay kits for each AU480 Biochemistry Analyzer (Beckman Coulter), following the manufacturer's protocols.

## Histopathological Assessment of the Ankle–Knee Joint

The joint tissue samples were fixed with 4% paraformaldehyde and then decalcified using nitric oxide. After gross examination, the histological samples were embedded in paraffin blocks and cut into 4- $\mu$ m-thin sections using a microtome<sup>38</sup> for subsequent analyses.

## H& E Staining

H&E staining was performed following the methods described in previous studies.<sup>39,40</sup> The tissue sections were deparaffinized on coated slides using absolute xylene (100%) and rehydrated using ethyl alcohol series from 100% to 70%. After washing with distilled water, the slides were incubated in hematoxylin solution for 10 min (depending on the nature of the hematoxylin stain). The hematoxylin stain was recycled, and the slides were placed under low-speed tap water and subsequently dipped once for gentle treatment with 1% HCl and 1% ammonia water. The slides were incubated with eosin and then air-dried. The dried slides were processed using a dehydration protocol and covered with glass coverslips. Images were captured using an Olympus microscope (Olympus Co. Ltd., Tokyo, Japan), specifically checking for aggregated inflammatory cells, degenerated muscle cells, and synovial fluid. The microscopic images were analyzed using ImageJ software (NIH, Bethesda, MD, USA).<sup>41</sup>

## Immunohistochemical Analysis

With slight modifications, immunohistochemical staining was performed as previously described.<sup>42</sup> To retrieve the antigen, the slides were subjected to proteinase K treatment and washed with PBS, and the peroxidase activity was quenched. The slides were blocked with normal goat serum (NGS) and incubated overnight with mouse anti-nuclear factor- $\kappa$ B (p-NF- $\kappa$ B) and mouse anti-TNF- $\alpha$  (1:100; Santa Cruz Biotechnology). After washing, the secondary antibodies (1:50) were applied in a humidified chamber, followed by the ABC reagents (Santa Cruz Biotechnology). After washing, the slides were stained with DAB and then mounted using DPX. ImageJ software (NIH) was used to quantitatively evaluate the hyper-activated TNF- $\alpha$  and NF- $\kappa$ B. The total area was calculated by optimizing the TNF- $\alpha$  and NF- $\kappa$ B threshold intensity in the positive cells.

## Oxidative Enzymes Analysis

Stress markers glutathione (GSH) and glutathione s-transferase (GST) are generally used to measure oxidative damage and the relative effect of the test compounds. Phenylmethylsulfonyl fluoride (PMSF) was applied to freshly cut and homogenized (0.1M PBS at pH 7.4) brain tissue samples and centrifuged (4000 X g) at 4 °C for 10 minutes. The supernatant layer was collected to evaluate the GSH levels using the already reported method with little modifications. To dissolve 0.6 mM DTNB, 0.2 M of sodium phosphate solution was used and 2 mL of this subsequent mixture was added to 0.2 mL of already collected supernatant. In order to collect a 3 mL solution, the final volume makeup was done with 0.2 M PBS. After 10 min, the absorbance of the test mixture was determined at a wavelength of 412 nm. As a negative and positive control, the phosphate buffer and DTNB solution were used respectively, which were further used to correct the measured absorbance. The results obtained were expressed in  $\mu$ moles/mg of proteins. Glutathione s-transferase (GST) marker levels have also been determined using a previously documented protocol with little modifications.<sup>43</sup> To prepare a test solution containing 5 mM GSH and 1 mM CDNB, a freshly prepared 0.1 M PBS was used. In a glass vial containing 1.2 mL of test solution in triplicate, 60  $\mu$ L of the already separated supernatant layer was added. Water was also used to prepare blanks in triplicate in the same proportion. These prepared solutions (210  $\mu$ L) were added to the microtiter plate and the ELISA microplate reader was used to detect the absorbance ( $\lambda_{\max}$  = 340 nm, 5 min at 23°C). Likewise, the values obtained were expressed in  $\mu$ moles/mg of proteins. Catalase (CAT) is a common heme-containing enzyme that catalyzes the decomposition of H<sub>2</sub>O<sub>2</sub> to H<sub>2</sub>O. Catalase activity was measured by monitoring the decrease in absorbance due to decomposition of H<sub>2</sub>O<sub>2</sub> at 240 nm according to the previously reported method with minor modifications.<sup>44</sup> A reaction mixture consisting of 1.95 mL of PBS (pH 7.0), 1mL of hydrogen peroxide (H<sub>2</sub>O<sub>2</sub>), and 0.05mL of supernatant was prepared and the absorbance was measured at 240 nm. The results were expressed as  $\mu$ moles of H<sub>2</sub>O<sub>2</sub>/min/mg of protein.

## Assessment of LPO in the Joint Tissues

A previously published method was used to evaluate LPO.<sup>44</sup> The rat joint tissue was homogenized in 20 mM Tris-HCl using a polytron homogenizer. Following supernatant collection, ferrous ammonium sulfate was added to the clear supernatant, and the mixture was incubated at 37 °C to calculate LPO. Subsequently, 2-thiobarbituric acid (TBA) was added to the mixture, and the absorbance was calculated at 532 nm using a microplate reader.

## ELISA

The levels of NLPR3 and TNF- $\alpha$  in the joint tissues were determined using the rat NLPR3 and TNF- $\alpha$  ELISA kits, following the manufacturers' instructions. The samples were homogenized in PBS at 15,000 RPM, and the supernatant was collected. The total protein concentration was quantified using the BCA method (Elabscience), while the concentrations of NLPR3 and TNF- $\alpha$  were measured using the ELx808 ELISA microplate reader (Bio-Tek Instruments, Winooski, VT, USA). The concentrations (pg/mL) were subsequently normalized to the total protein content (pg/mg).

## Statistical Analysis

The data were expressed as means  $\pm$  standard error of the mean (SEM) and analyzed via one-way analysis of variance (ANOVA), followed by Tukey's post-hoc test, using GraphPad Prism software (GraphPad, San Diego, CA, USA). Statistical significance was set at  $p < 0.05$ . The symbol # shows a significant difference relative to the saline group, and \* shows a significant difference relative to the PO group.

## Results

### Effects of Carvacrol Treatment on the Serum Biochemistry Profile of Hyperuricemic Rats

The effects of daily intraperitoneal administration of carvacrol for seven consecutive days in normal and PO-induced hyperuricemic rats are presented in Table 1. Compared to the normal group, the model group exhibited significantly increased serum uric acid and CRP levels ( $p < 0.001$ ), indicating the successful induction of hyperuricemia in rats.<sup>45</sup> A comparison between hyperuricemia and allopurinol-treated rats also showed a significant decrease in the serum uric acid and CRP levels ( $p < 0.001$ ). The groups treated with different doses of carvacrol (20 and 50 mg/kg) presented similar results ( $p < 0.001$ ), but a slightly pronounced effect was observed on the serum uric acid level of the carvacrol 50 group. The anti-inflammatory effect of carvacrol was also observed in both groups, as evidenced by the reduced serum CRP levels. In addition, to assess the relative safety of carvacrol treatments on the rat kidneys, we measured the serum creatinine levels and found no renal impairment at the utilized dosages.

**Table 1** Effects of Carvacrol and Allopurinol Treatments (n = 7 per Group) on the Serum Levels of Urea, Creatinine, Uric Acid, and CRP in PO-Induced Hyperuricemic Rats

Treatment	Urea (mg/dl)	Creatinine (mg/dl)	Uric Acid (mg/dl)	CRP (mg/L)
Baseline	25.86 $\pm$ 0.79	0.276 $\pm$ 0.03	2.83 $\pm$ 0.04	1.17 $\pm$ 0.11
Saline	26.40 $\pm$ 0.87	0.29 $\pm$ 0.04	2.91 $\pm$ 0.053	1.3 $\pm$ 0.1
PO model 250mg/kg	32.0 $\pm$ 0.9 <sup>###</sup>	0.379 $\pm$ 0.02 <sup>###</sup>	7.19 $\pm$ 0.33 <sup>####</sup>	28.6 $\pm$ 1.52 <sup>####</sup>
Allopurinol 10mg/kg	28.67 $\pm$ 0.88	0.303 $\pm$ 0.008	2.53 $\pm$ 0.29 <sup>***</sup>	1.63 $\pm$ 0.12 <sup>***</sup>
Carvacrol 20	20.75 $\pm$ 0.48 <sup>***</sup>	0.305 $\pm$ 0.04	2.43 $\pm$ 0.11 <sup>***</sup>	1.77 $\pm$ 0.15 <sup>***</sup>
Carvacrol 50	19.75 $\pm$ 0.63 <sup>***</sup>	0.33 $\pm$ 0.04	2.01 $\pm$ 0.57 <sup>***</sup>	1.75 $\pm$ 0.15 <sup>***</sup>

**Notes:** PO (250 mg/kg) was administered to induce gout in the model group. Saline-treated rats were considered as the control group, while allopurinol-treated rats were used as the standard group. The data are presented as means  $\pm$  SEM. <sup>####</sup> $p < 0.001$  and <sup>###</sup> $p < 0.01$  vs saline group, <sup>\*\*\*</sup> $p < 0.001$  vs model group. Mean values with dissimilar superscripts in a column significantly vary at  $p < 0.05$ .

**Abbreviations:** CRP, C-reactive protein; PO, potassium oxonate.

## Carvacrol Treatment Ameliorates Renal and Joint Degeneration in Hyperuricemic Rats

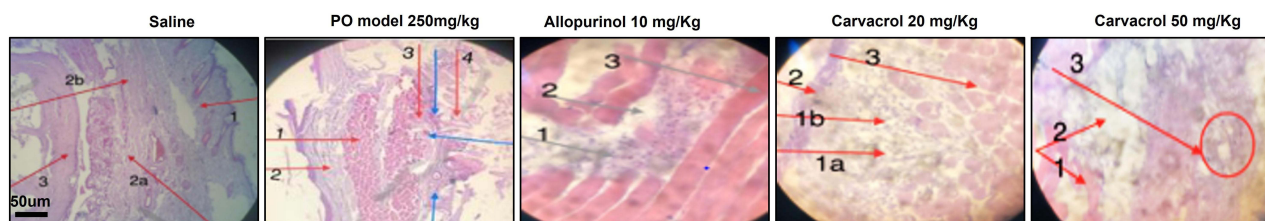
Compared to the saline group, which showed no pathological changes and normal architecture of the joint tissues, significant alterations were observed in the PO group, including large pale areas with giant cells and abundant MSU crystals in both the intracellular and extracellular spaces, indicating the presence of gout (Figure 1, Table 2). Furthermore, a moderate amount of inflammatory cells, which can lead to inflammation and edema formation, were observed in the carvacrol 20 group. Notably, there were no inflammatory cells, MSU crystals, spared skin, and muscle cells in the carvacrol 50 group, indicating normal architecture of the joint tissues. In contrast, a small number of inflammatory cells was observed in the allopurinol group, but there were no MSU crystals in the intracellular and extracellular spaces. The renal function test revealed no significant cellular changes, thus validating the safety and non-hazardous effect of carvacrol treatment on rat kidneys.

## Carvacrol Treatment Reduces the Levels of Inflammatory Cytokines in Hyperuricemic Rats

The concentration of NLRP3 in the tissues surrounding the rat knee joints was determined using ELISA. Compared to the baseline expression (day 1 of treatment), the level of NLRP3 at day 7 was significantly enhanced in the model group ( $p < 0.01$ , Figure 2A). In contrast, the NLRP3 levels in the allopurinol- and carvacrol-treated groups (20 and 50 mg/kg) were significantly reduced at day 7 ( $p < 0.05$ ). Since NLRP3 is associated with downstream inflammatory cytokines, we also investigated the effects of carvacrol treatment on the TNF- $\alpha$  and p-NF $\kappa$ B levels. Notably, we observed that the level of TNF- $\alpha$  was significantly higher in the model group than in the saline group ( $p < 0.001$ , Figure 2B). However, the carvacrol treatment attenuated the PO-induced increase in TNF- $\alpha$  level in hyperuricemic rats. For validation, we performed immunohistochemical analysis and observed similar results (Figure 2C). We also performed immunohistochemistry for p-NF $\kappa$ B and found that carvacrol attenuated the p-NF $\kappa$ B level in the model group ( $p < 0.001$ , Figure 2D).

## Effects of Carvacrol Treatment on the Levels of Oxidative Stress Mediators in Hyperuricemic Rats

As early indicators of oxidative damage, the levels of enzymatic and non-enzymatic oxidants, namely GST and GSH, were measured in the joint tissues. The administration of PO-induced ROS coincided with the exhaustion of GSH and GST in the joint tissue homogenates of the model group (Figure 3A and B). In contrast, treatment with carvacrol (20 and 50 mg/kg) resulted in increased GSH and GST levels and restored CAT levels in the joint tissue homogenates (Figure 3C). The oxidative stress and ROS generated in hyperuricemia generally induce the formation of several detrimental products (eg, malondialdehyde) that can be measured using the thiobarbituric acid reactive substances (TBARS) assay. The LPO assay



Joint tissue

**Figure 1** Effects of carvacrol treatment on the morphological integrity of the joint tissues in PO-induced hyperuricemic rats. The joint tissues ( $n = 7$  per group) were stained with H&E and then observed under  $10\times$  magnification. Scale bar =  $50\ \mu\text{m}$ . Saline group: 1, skin tissue; 2a and 2b, synovial fluid, 3, muscle tissue. Model group (PO treatment): 1 indicates muscle; 2 indicates skin; 3 indicates urate crystals. Blue arrows indicate inflammatory cells. Allopurinol group (10 mg/kg allopurinol treatment): 1 indicates inflammatory plasma cells (lymphocytes); 2 indicates synovial fluid; 3 indicates muscle cell. Carvacrol 20 group (20 mg/kg carvacrol treatment): 1a and 1b are moderate inflammation (acute and chronic); 2 indicates skin; 3 indicates muscle. Carvacrol 50 group (50 mg/kg carvacrol treatment): 1 indicates muscle; 2 indicates skin; 3 indicates inflammatory cells (encircled).

**Table 2** Effects of Carvacrol Treatment on the Inflammatory Mediators of PO-Induced Hyperuricemic Rats

Groups	MSUC (Shown by Blue Arrows)	Inflammatory Cells- Lymphocytes (Shown by Blue Arrows)	Synovial Fluid (Shown by Red Arrows)	Skin/Muscle (Shown by Red Arrows)
Saline	0	0		
PO model 250mg/kg	3	2	0	
Allopurinol 10mg/kg	2			
Carvacrol 20mg	0			
Carvacrol 50mg	0	0		

**Notes:** 0 indicates absence; | indicates presence; 2 indicates >10 particles per field; 3 indicates >20 particles per field.

revealed that compared to the saline group, there was an increase in the levels of LPO products in the model group, suggesting a high degree of LPO-induced damage in the joint tissue (Figure 3D). Notably, treatment with carvacrol and allopurinol both reduced the LPO-induced damages in the joint tissues of hyperuricemic rats.

## Discussion

In the present study, we investigated the effects of carvacrol on the oxidative and inflammatory cascades of hyperuricemic rats and obtained results corroborating those of previous studies.<sup>46,47</sup> We further evaluated the positive effects of carvacrol treatment and observed a dose-dependent response in the carvacrol-treated groups, with results comparable to those of allopurinol-treated rats. Natural drugs, such as carvacrol, are extensively investigated for their great pharmacological potential against various diseases, specifically for elucidating the underlying disease pathology and developing newer and safer therapeutic alternatives. Notably, previous studies discovered that carvacrol is a dietary adjuvant that can ameliorate gout-like symptoms.<sup>48,49</sup> Here, we successfully induced hyperuricemia in rats using PO, which was validated

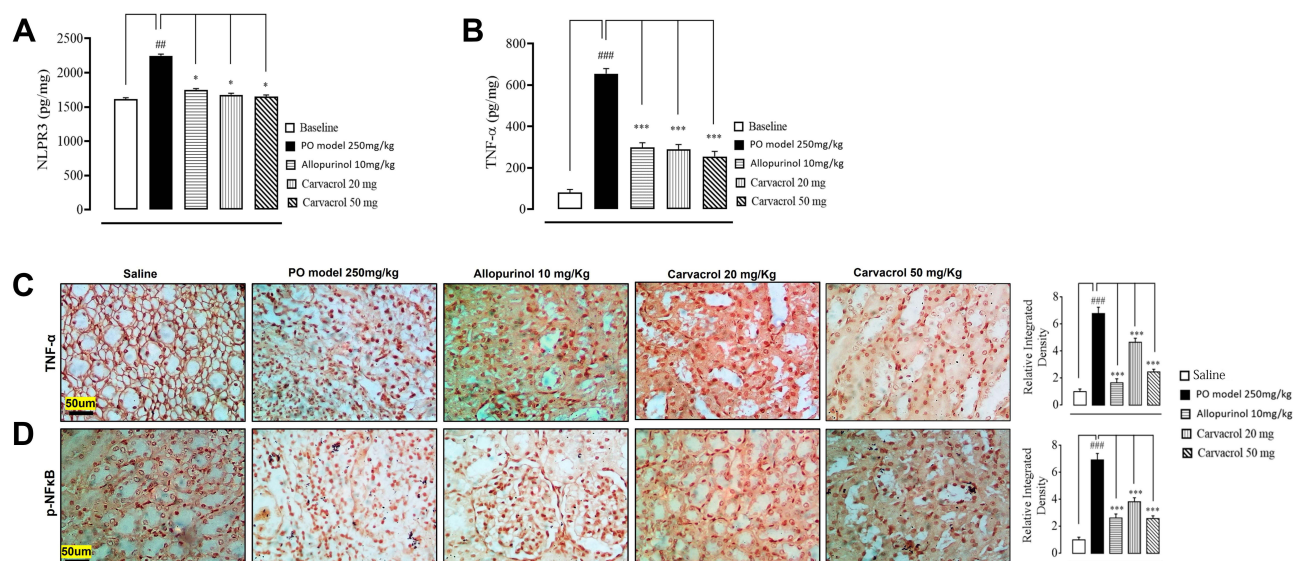


**Figure 2** Effects of carvacrol treatment on the inflammatory mediators of PO-induced hyperuricemic rats. The tissue levels of (A) NLRP3 and (B) TNF- $\alpha$  were quantified using ELISA (n = 7 per group). The data are presented as means  $\pm$  SEM. Representative images showing the immunoreactivity of (C) TNF- $\alpha$  (D) p-NF- $\kappa$ B (n = 7 per group). Scale bar = 50  $\mu$ m, 40 $\times$  magnification. The data are presented as means  $\pm$  SEM. \*\*\* $p$  < 0.001 compared to the model group (PO treated), #### $p$  < 0.001 compared to the saline group, ## $p$  < 0.01 compared to the saline group, \* $p$  < 0.05 compared to the model group (PO treated).

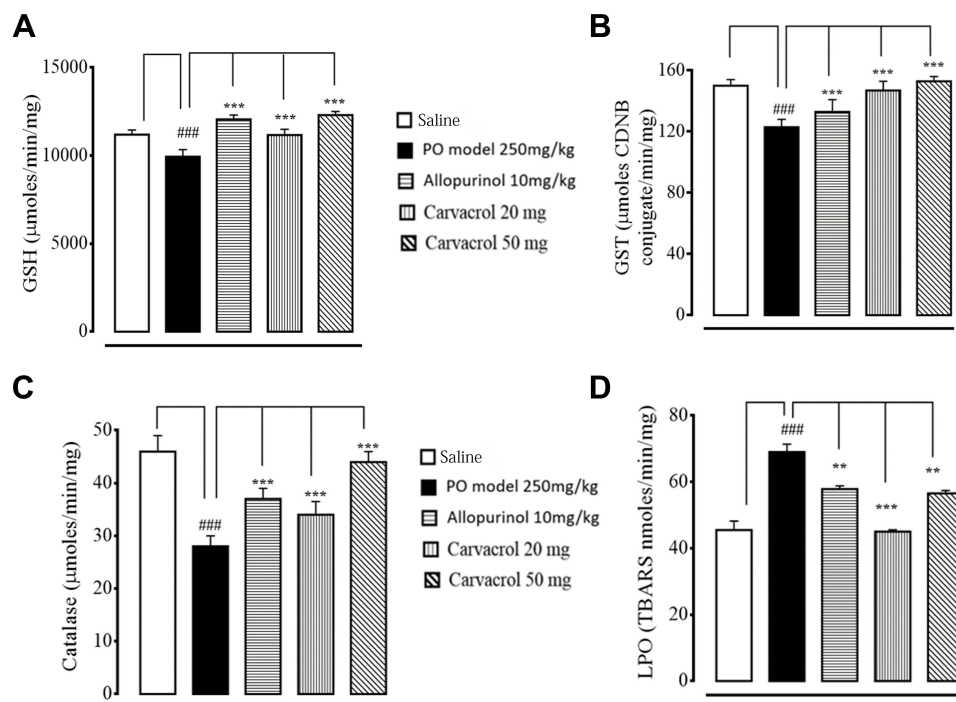


**Figure 3** Effects of carvacrol and allopurinol treatments on the enzymatic and non-enzymatic oxidants of PO-induced hyperuricemic rats. The enzymatic activities of (A) GSH, (B) GST, (C) CAT, and (D) LPO were measured. The data are presented as means  $\pm$  SEM. ### $p$  < 0.001 compared to the saline group, \*\*\* $p$  < 0.001 compared to the model group (PO-treated), \*\* $p$  < 0.01 compared to the model group (PO-treated).

**Abbreviations:** PO, potassium oxonate; CAT, catalase; GSH, reduced glutathione; GST, glutathione-S-transferase; LPO, lipid peroxidation.

by the high serum uric acid and CRP levels.<sup>45</sup> We also found that carvacrol treatment attenuated the levels of both serum CRP and TNF- $\alpha$  in the joint tissues of hyperuricemic rats.

Several studies suggested that the hyperactivity of xanthine oxidase is a contributing factor of hyperuricemia that triggers uric acid overproduction, which is mainly concentrated in the limbs.<sup>50</sup> Moreover, the early phase of inflammation starts with immune cell infiltration into the gouty tissue, inducing the release of inflammatory cytokines (eg, IL-1 $\beta$ , IL-6, and TNF- $\alpha$ ).<sup>15,19</sup> This subsequently exacerbates the inflammatory reactions and leads to tissue destruction.<sup>51,52</sup> In addition, the deposition of MSU crystals in the joint tissue reportedly aggravates the pathological cascade of gout by activating the NLRP3 inflammasome,<sup>53</sup> which modulates the release of inflammatory mediators and cytokines (eg, COX2 and p-NF- $\kappa$ B), thus further aggravating the pathological cascade. We also investigated the role of the NLRP3 inflammasome and its mediators and discovered that the inflammation-related markers can exacerbate pathogenicity in the model group, while carvacrol treatment reduced the levels of both MSU crystals and inflammatory mediators. However, the exact mechanism underlying the anti-inflammatory effects of carvacrol requires further research. Notably, our findings corroborate previous observations,<sup>54,55</sup> wherein targeting the NLRP3 inflammasome can modulate MSU crystal deposition. Moreover, enhanced neutrophil permeation into the intraarticular and periarticular spaces during gout can induce severe pain due to edema and erythema formation.<sup>56</sup> Furthermore, dysfunction in the NLRP3 assembly impairs the neutrophil influx into the gouty tissue, suggesting the critical involvement of NLRP3 in gouty arthritis.<sup>57</sup> Additionally, B-hydroxybutyrate prevents NLRP3 inflammasome activation and MSU crystal deposition by downregulating NLRP3 expression.<sup>55</sup> Recent studies have identified several therapeutic targets, including chemokines, TNF- $\alpha$ , and NLRP3 inflammasomes, and correspondingly developed different anti-inflammatory strategies against gout.<sup>58,59</sup> Therefore, directly targeting NLRP3 and its associated factors or proteins may effectively inhibit NLRP3 activation and potentially produce benefits in gout treatment.<sup>60</sup> Previous clinical trials utilizing different drugs that target only a single step in a specific disorder have failed. However, in this study, carvacrol ameliorated the detrimental effects of hyperuricemia by targeting multiple stages, including inflammation, oxidative stress, and cellular degeneration. Hence, our results demonstrate that

a natural drug with protective effects that can act against different stages of pathogenesis may be more effective for clinical applications.

The use of urate-lowering agents are often associated with renal injuries, thus limiting their applications in renal-compromised patients.<sup>61</sup> Here, we demonstrate the renal safety of carvacrol that was not previously observed with other natural compounds, such as polydatin, which decreases the serum uric acid level but increases the serum creatinine level, thereby indicating abnormal metabolic status in hyperuricemic rats.<sup>62</sup> In addition, carvacrol exhibited a relative safety profile because no impairment was observed in the kidneys. The serum creatinine and urea levels were also normal and similar to previous findings.<sup>63</sup> Serum uric acid reportedly accumulates in the peripheral joints as MSU crystals. However, the crystals spontaneously dissolve when uric acid concentrations fall below the saturation level of MSU crystals, and thus, gout can be resolved.<sup>7</sup> Here, the carvacrol treatment effectively reduced the serum uric acid level, as confirmed by the low number of crystal aggregates observed during morphological analysis.

Since inflammation is a key factor in gout pathogenesis, compounds exhibiting both anti-hyperuricemic and anti-inflammatory activities are essential for developing treatment strategies for gout.<sup>64</sup> However, currently available medications exert considerable anti-hyperuricemic effects but have poor anti-inflammatory potential. Notably, our histopathological findings revealed that different doses of carvacrol can inhibit the accumulation of inflammatory cells in both the connective and muscle tissues, thereby confirming its effective anti-inflammatory activity. Overall, our findings suggest that carvacrol has great therapeutic potential because the significant decrease in serum uric acid level was accompanied by reduced inflammation in the joint tissues, and these effects did not produce toxicity to the rat kidneys.

## Conclusions

Taken together, we can conclude from our results that carvacrol possesses antioxidant and anti-inflammatory properties and ameliorated the gout symptoms in hyperuricemic rats in a dose-dependent manner. Further, our proposed mechanism suggests that carvacrol activated the endogenous antioxidant proteins like GSH, GST, and catalase coupled to the downregulation of anti-inflammatory proteins like p-NF $\kappa$ B and NLRP3 (Figure 4). Collectively, these protective properties of carvacrol may offer a new therapeutic option for protecting the joint tissues from inflammation and oxidative stress-induced degeneration.

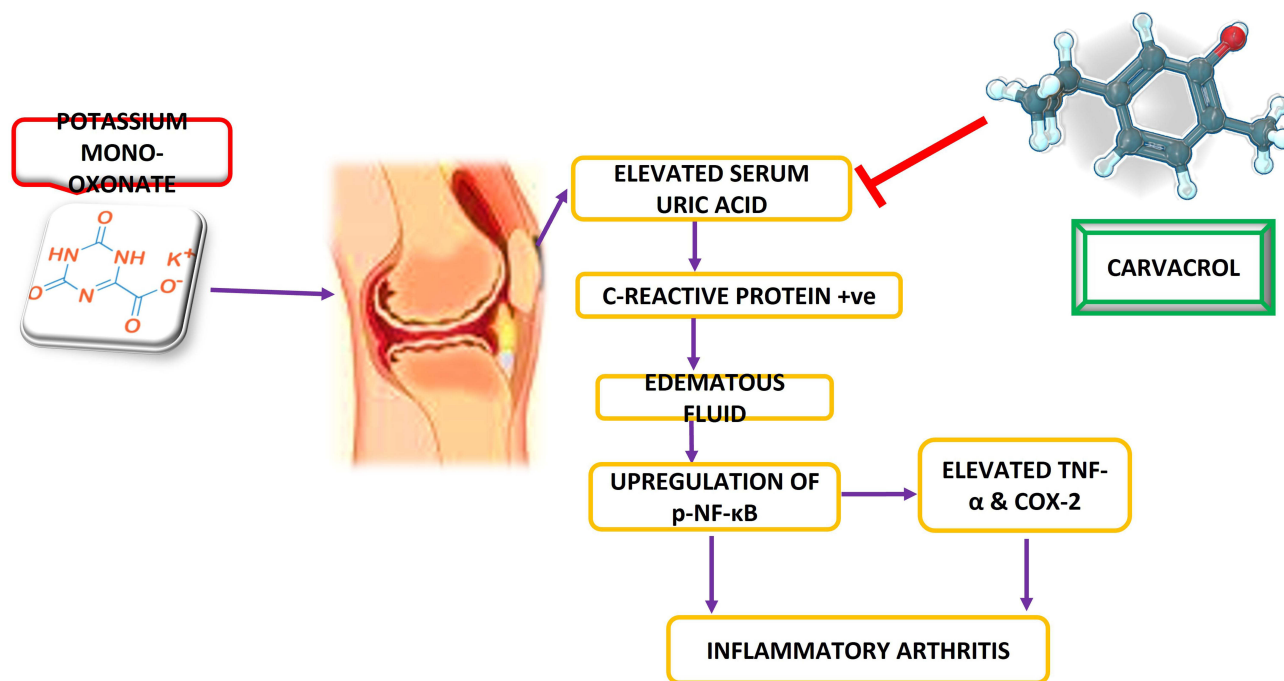


**Figure 4** Diagrammatic illustration elaborating the underlying antioxidant and neuroprotective potential of carvacrol in a PO-induced gout model.

## Ethics Approval

The study was conducted and approved by the Institutional Review Board (or Ethics Committee) of Riphah Institute of Pharmaceutical Sciences, Riphah International University.

## Author Contributions

All authors made a significant contribution to the work reported, whether that is in the conception, study design, execution, acquisition of data, analysis and interpretation, or in all these areas; took part in drafting, revising or critically reviewing the article; gave final approval of the version to be published; have agreed on the journal to which the article has been submitted; and agree to be accountable for all aspects of the work.

## Funding

This research was funded by ORIC grant number 12134454, Riphah International University.

## Disclosure

The authors declare no conflict of interest.

## References

1. Becker MA, Schumacher HR Jr, Wortmann RL, et al. Febuxostat compared with allopurinol in patients with hyperuricemia and gout. *N Engl J Med*. 2005;353(23):2450–2461. doi:10.1056/NEJMoa050373
2. Chatzipavlou M, Magiorkinis G, Koutsogeorgopoulou L, Kassimos D. Mediterranean diet intervention for patients with hyperuricemia: a pilot study. *Rheumatol Int*. 2014;34(6):759–762. doi:10.1007/s00296-013-2690-7
3. Dehlin M, Jacobsson L, Roddy E. Global epidemiology of gout: prevalence, incidence, treatment patterns and risk factors. *Nat Rev Rheumatol*. 2020;16(7):380–390. doi:10.1038/s41584-020-0441-1
4. Ashiq K, Bajwa MA, Tanveer S, et al. A comprehensive review on gout: the epidemiological trends, pathophysiology, clinical presentation, diagnosis and treatment. *J PMA*. 2021;4:71.
5. Chiou A, England BR, Sayles H, et al. Coexistent hyperuricemia and gout in rheumatoid arthritis: associations with comorbidities, disease activity, and mortality. *Arthritis Care Res*. 2020;72(7):950–958. doi:10.1002/acr.23926
6. Li L, Zhang Y, Zeng C. Update on the epidemiology, genetics, and therapeutic options of hyperuricemia. *Am J Transl Res*. 2020;12(7):3167–3181.
7. Martillo MA, Nazzal L, Crittenden DB. The crystallization of monosodium urate. *Curr Rheumatol Rep*. 2014;16(2):400. doi:10.1007/s11926-013-0400-9
8. Cho J, Kim C, Kang DR, Park JB. Hyperuricemia and uncontrolled hypertension in treated hypertensive patients: k-MetS Study. *Medicine*. 2016;95(28):28. doi:10.1097/MD.00000000000004177
9. Shah P, Bjornstad P, Johnson RJ. Hyperuricemia as a potential risk factor for type 2 diabetes and diabetic nephropathy. *SciELO Bras*. 2016;4:56.
10. Zoppini G, Targher G, Concholl M, et al. Serum uric acid levels and incident chronic kidney disease in patients with type 2 diabetes and preserved kidney function. *Diabetes Care*. 2012;35(1):99–104. doi:10.2337/dc11-1346
11. Ogura T, Matsuura K, Matsumoto Y, et al. Recent trends of hyperuricemia and obesity in Japanese male adolescents, 1991 through 2002. *Metabolism*. 2004;53(4):448–453. doi:10.1016/j.metabol.2003.11.017
12. Yokokawa H, Fukuda H, Suzuki A, et al. Association between serum uric acid levels/hyperuricemia and hypertension among 85,286 Japanese workers. *J Clin Hypertens*. 2016;18(1):53–59. doi:10.1111/jch.12627
13. Sattui SE, Gaffo AL. Treatment of hyperuricemia in gout: current therapeutic options, latest developments and clinical implications. *Ther Adv Musculoskelet Dis*. 2016;8(4):145–159. doi:10.1177/1759720X16646703
14. Benn CL, Dua P, Gurrell R, et al. Physiology of hyperuricemia and urate-lowering treatments. *Front med*. 2018;5:160. doi:10.3389/fmed.2018.00160
15. Dalbeth N, Haskard D. Mechanisms of inflammation in gout. *Rheumatology*. 2005;44(9):1090–1096. doi:10.1093/rheumatology/keh640
16. Filipe P, Haigle J, Freitas J, et al. Anti-and pro-oxidant effects of urate in copper-induced low-density lipoprotein oxidation. *Eur J Biochem*. 2002;269(22):5474–5483. doi:10.1046/j.1432-1033.2002.03245.x
17. Aruoma OL, Halliwell B. Inactivation of  $\alpha$ 1-antiproteinase by hydroxyl radicals The effect of uric acid. *FEBS Lett*. 1989;244(1):76–80. doi:10.1016/0014-5793(89)81166-4
18. Martinon F. Mechanisms of uric acid crystal-mediated autoinflammation. *Immunol Rev*. 2010;233(1):218–232. doi:10.1111/j.0105-2896.2009.00860.x
19. Busso N, Gout SA. Mechanisms of inflammation in gout. *Arthritis Res Ther*. 2010;12(2):1–8. doi:10.1186/ar2952
20. Latz E, Xiao TS, Stutz A. Activation and regulation of the inflammasomes. *Nat Rev Immunol*. 2013;13(6):397–411. doi:10.1038/nri3452
21. Szekanecz Z, Szamosi S, Kovács GE, Kocsis E, Benkő S. The NLRP3 inflammasome-interleukin 1 pathway as a therapeutic target in gout. *Arch Biochem Biophys*. 2019;670:82–93. doi:10.1016/j.abb.2019.01.031
22. Wang Z, Zhang S, Xiao Y, et al. NLRP3 inflammasome and inflammatory diseases. *Oxid Med Cell Longev*. 2020;2020:e45.
23. Chen L, Lan Z. Polydatin attenuates potassium oxonate-induced hyperuricemia and kidney inflammation by inhibiting NF- $\kappa$ B/NLRP3 inflammasome activation via the AMPK/SIRT1 pathway. *Food Funct*. 2017;8(5):1785–1792. doi:10.1039/C6FO01561A
24. Deng W, Yang Z, Yue H, Ou Y, Hu W, Sun P. Disulfiram suppresses NLRP3 inflammasome activation to treat peritoneal and gouty inflammation. *Free Radic Biol Med*. 2020;152:8–17. doi:10.1016/j.freeradbiomed.2020.03.007

25. Klück V, Tim L, Janssen M, et al. Dapansutrile, an oral selective NLRP3 inflammasome inhibitor, for treatment of gout flares: an open-label, dose-adaptive, proof-of-concept, phase 2a trial. *Lancet Rheumatol*. 2020;2(5):e270–e280. doi:10.1016/S2665-9913(20)30065-5
26. Liu X, Chen R, Shang Y, Jiao B, Huang C. Lithospermic acid as a novel xanthine oxidase inhibitor has anti-inflammatory and hypouricemic effects in rats. *Chem Biol Interact*. 2008;176(2–3):137–142. doi:10.1016/j.cbi.2008.07.003
27. Liu Y, Tang H, Liu X, et al. Frontline Science: reprogramming COX-2, 5-LOX, and CYP4A-mediated arachidonic acid metabolism in macrophages by salidroside alleviates gouty arthritis. *J Leukoc Biol*. 2019;105(1):11–24. doi:10.1002/JLB.3HI0518-193R
28. Kiyani MM, Butt MA, Rehman H, et al. Antioxidant and anti-gout effects of orally administered zinc oxide nanoparticles in gouty mice. *J Trace Elem Med Biol*. 2019;56:169–177. doi:10.1016/j.jtemb.2019.08.012
29. Kiyani MM, Butt MA, Rehman H, et al. Evaluation of antioxidant activity and histopathological changes occurred by the oral ingestion of CuO nanoparticles in monosodium urate crystal-induced hyperuricemic BALB/c mice. *Biol Trace Elem Res*. 2000;2022:217–227.
30. Malik I, Shah FA, Ali T, et al. Potent natural antioxidant carveol attenuates MCAO-stress induced oxidative, neurodegeneration by regulating the Nrf-2 pathway. *Front Neurosci*. 2020;14:659. doi:10.3389/fnins.2020.00659
31. Al Kury LT, Dayyan F, Ali Shah F, et al. Ginkgo biloba extract protects against methotrexate-induced hepatotoxicity: a computational and pharmacological approach. *Molecules*. 2020;25(11):2540. doi:10.3390/molecules25112540
32. Shah FA, Kury LA, Li T, et al. Polydatin attenuates neuronal loss via reducing neuroinflammation and oxidative stress in rat MCAO models. *Front Pharmacol*. 2019;10:663. doi:10.3389/fphar.2019.00663
33. Sharifi-Rad M, Varoni EM, Iriti M, et al. Carvacrol and human health: a comprehensive review. *Phytother Res*. 2018;32(9):1675–1687. doi:10.1002/ptr.6103
34. Bayir AG, Kiziltan HS, Kocyigit A. Plant family, carvacrol, and putative protection in gastric cancer. In: *Dietary Interventions in Gastrointestinal Diseases*. Elsevier; 2019:3–18.
35. Wang X, Wang C-P, Hu Q-H, et al. The dual actions of Sanmiao wan as a hypouricemic agent: down-regulation of hepatic XOD and renal mURAT1 in hyperuricemic mice. *J Ethnopharmacol*. 2010;128(1):107–115. doi:10.1016/j.jep.2009.12.035
36. Oh DR, Kim JR, Choi CY, et al. Effects of ChondroT on potassium Oxonate-induced Hyperuricemic mice: downregulation of xanthine oxidase and urate transporter 1. *BMC Complement Altern Med*. 2019;19(1):10. doi:10.1186/s12906-018-2415-2
37. Ullah U, Badshah H, Malik Z, et al. Hepatoprotective effects of melatonin and celecoxib against ethanol-induced hepatotoxicity in rats. *Immunopharmacol Immunotoxicol*. 2020;42(3):255–263. doi:10.1080/08923973.2020.1746802
38. Imran M, Shah FA, Nadeem H, et al. Synthesis and biological evaluation of benzimidazole derivatives as potential neuroprotective agents in an ethanol-induced rodent model. *ACS Chem Neurosci*. 2021;12(3):489–505. doi:10.1021/acscchemneuro.0c00659
39. Mohsin Alvi A, Tariq Al Kury L, Umar Ijaz M, et al. Post-treatment of synthetic polyphenolic 1, 3, 4 oxadiazole compound A3, attenuated ischemic stroke-induced neuroinflammation and neurodegeneration. *Biomolecules*. 2020;10(6):816. doi:10.3390/biom10060816
40. Ali A, Shah FA, Zeb A, et al. NF-κB inhibitors attenuate MCAO induced neurodegeneration and oxidative stress—a reprofiling approach. *Front Mol Neurosci*. 2020;13:33. doi:10.3389/fnmol.2020.00033
41. Imran M, Al Kury LT, Nadeem H, et al. Benzimidazole containing acetamide derivatives attenuate neuroinflammation and oxidative stress in ethanol-induced neurodegeneration. *Biomolecules*. 2020;10(1):108. doi:10.3390/biom10010108
42. Iqbal S, Shah FA, Naeem K, et al. Succinamide derivatives ameliorate neuroinflammation and oxidative stress in scopolamine-induced neurodegeneration. *Biomolecules*. 2020;10(3):443. doi:10.3390/biom10030443
43. Zulfiqar Z, Shah FA, Shafique S, et al. Repurposing FDA approved drugs as JNK3 inhibitor for prevention of neuroinflammation induced by MCAO in rats. *J Inflamm Res*. 2020;13:1185. doi:10.2147/JIR.S284471
44. Rahman ZU, Al Kury LT, Alattar A, et al. Carveol a naturally-derived potent and emerging nrf2 activator protects against Acetaminophen-induced hepatotoxicity. *Front Pharmacol*. 2020;11:e34.
45. Neogi T, Jansen TL, Dalbeth N, et al. Gout classification criteria: an American College of Rheumatology/European league against rheumatism collaborative initiative. *Arthritis Rheumatol*. 2015;67(10):2557–2568. doi:10.1002/art.39254
46. Guimarães AG, Xavier MA, de Santana MT, et al. Carvacrol attenuates mechanical hypernociception and inflammatory response. *Naunyn-Schmiedeberg's Arch Pharmacol*. 2012;385(3):253–263. doi:10.1007/s00210-011-0715-x
47. Silva FV, Guimarães AG, Silva ER, et al. Anti-inflammatory and anti-ulcer activities of carvacrol, a monoterpene present in the essential oil of oregano. *J Med Food*. 2012;15(11):984–991. doi:10.1089/jmf.2012.0102
48. Rezaeinasab M, Benvidi A, Gharaghani S, Abbasi S, Zare HR. Electrochemical investigation of the inhibition effect of carvacrol on xanthine oxidase activity merging with theoretical studies. *Process Biochem*. 2019;83:86–95. doi:10.1016/j.procbio.2019.03.014
49. da Silva Lima M, Quintans-Júnior LJ, de Santana WA, Kaneto CM, Soares MBP, Villarreal CF. Anti-inflammatory effects of carvacrol: evidence for a key role of interleukin-10. *Eur J Pharmacol*. 2013;699(1–3):112–117. doi:10.1016/j.ejphar.2012.11.040
50. Kiyani MM, Moghul NB, Butt MA, et al. Anti-hyperuricemic effect of iron oxide nanoparticles against monosodium urate crystals induced gouty arthritis in BALB/c mice. *Biol Trace Elem Res*. 2021;4:56.
51. Di Giovine FS, Malawista SE, Thornton E, Duff GW. Urate crystals stimulate production of tumor necrosis factor alpha from human blood monocytes and synovial cells. Cytokine mRNA and protein kinetics, and cellular distribution. *J Clin Invest*. 1991;87(4):1375–1381. doi:10.1172/JCI115142
52. Yagnik DR, Evans BJ, Florey O, Mason JC, Landis RC, Haskard DO. Macrophage release of transforming growth factor beta1 during resolution of monosodium urate monohydrate crystal-induced inflammation. *Arthritis Rheum*. 2004;50(7):2273–2280. doi:10.1002/art.20317
53. Kingsbury SR, Conaghan PG, McDermott MF. The role of the NLRP3 inflammasome in gout. *J Inflamm Res*. 2011;4:39. doi:10.2147/JIR.S11330
54. Coll RC, Robertson AA, Chae JJ, et al. A small-molecule inhibitor of the NLRP3 inflammasome for the treatment of inflammatory diseases. *Nat Med*. 2015;21(3):248–255. doi:10.1038/nm.3806
55. Youm Y-H, Nguyen KY, Grant RW, et al. The ketone metabolite β-hydroxybutyrate blocks NLRP3 inflammasome-mediated inflammatory disease. *Nat Med*. 2015;21(3):263–269. doi:10.1038/nm.3804
56. Guma M, Ronacher L, Liu-Bryan R, Takai S, Karin M, Caspase CM. 1-independent activation of interleukin-1beta in neutrophil-predominant inflammation. *Arthritis Rheum*. 2009;60(12):3642–3650. doi:10.1002/art.24959
57. Martinon F, Pétrilli V, Mayor A, Tardivel A, Tschopp J. Gout-associated uric acid crystals activate the NALP3 inflammasome. *Nature*. 2006;440(7081):237–241. doi:10.1038/nature04516

58. Gout TR. Novel therapies for treatment of gout and hyperuricemia. *Arthritis Res Ther.* 2009;11(4):1–11.
59. Pillinger MH, Mandell BF Therapeutic approaches in the treatment of gout. *Sem Arthritis Rheumatism.* 2020;50(3S):S24–S30.
60. Choi N, Yang G, Jang JH, et al. Loganin alleviates gout inflammation by suppressing nlrp3 inflammasome activation and mitochondrial damage. *Molecules.* 2021;26(4):1071. doi:10.3390/molecules26041071
61. Hande KR, Noone RM, Stone WJ. Severe allopurinol toxicity: description and guidelines for prevention in patients with renal insufficiency. *Am J Med.* 1984;76(1):47–56. doi:10.1016/0002-9343(84)90743-5
62. Han B, Gong M, Li Z, Qiu Y, Zou Z. NMR-based metabonomic study reveals intervention effects of polydatin on potassium oxonate-induced hyperuricemia in rats. *Oxid Med Cell Longev.* 2020;2020:1–10. doi:10.1155/2020/6943860
63. Ahmadvand H, Tavafi M, Asadollahi V, et al. Protective effect of carvedilol on renal functional and histopathological changes in gentamicin-induced-nephrotoxicity in rats; 2016.
64. Hilmi B, Asmahan M, Rosman A. Use of newly available febuxostat in a case of chronic tophaceous gout contraindicated to allopurinol and probenecid. *Med J Malaysia.* 2012;67(1):125.

## Drug Design, Development and Therapy

Dovepress

### Publish your work in this journal

Drug Design, Development and Therapy is an international, peer-reviewed open-access journal that spans the spectrum of drug design and development through to clinical applications. Clinical outcomes, patient safety, and programs for the development and effective, safe, and sustained use of medicines are a feature of the journal, which has also been accepted for indexing on PubMed Central. The manuscript management system is completely online and includes a very quick and fair peer-review system, which is all easy to use. Visit <http://www.dovepress.com/testimonials.php> to read real quotes from published authors.

Submit your manuscript here: <https://www.dovepress.com/drug-design-development-and-therapy-journal>